

Leptonic μ - and τ -decays: mass effects, polarization effects and $O(\alpha)$ radiative corrections

M. Fischer, S. Groote, J.G. Körner and M.C. Mauser

Institut für Physik, Johannes Gutenberg-Universität
Staudinger Weg 7, D-55099 Mainz, Germany

Abstract

We calculate the radiative corrections to the unpolarized and three polarized spectrum and rate functions in polarized μ -decays into polarized electrons. The new feature of our calculation is that we keep the mass of the final state electron finite. Analytical results are given for the energy spectrum and the polar angle distribution of the final state electron whose longitudinal polarization is calculated. We also provide analytical results on the integrated spectrum functions. We analyze the $m_e \rightarrow 0$ limit of our general results and investigate the quality of the $m_e \rightarrow 0$ approximation. In the $m_e \rightarrow 0$ case we discuss in some detail the role of the anomalous helicity flip contribution of the final electron which survives the $m_e \rightarrow 0$ limit. The results presented in this paper also apply to the leptonic decays of polarized τ -leptons for which we provide numerical results.

1 Introduction

While calculating the radiative QCD corrections to polarization effects in semileptonic decays of heavy quarks, where the full quark mass dependence was retained [1, 2], we came to realize that our results could also be gainfully employed in the corresponding weak leptonic decays of the μ - and τ -leptons¹. In most of the previous radiative correction calculations the mass of the charged lepton daughter l' has been neglected except for anomalous contributions from the collinear region which survive the $m'_l \rightarrow 0$ limit [3, 4, 5] and the logarithmic terms $\sim (\ln m'_l)$ which are needed to regularize the collinear divergencies that appear in the loop and tree graph (“internal bremsstrahlung”) contributions. These logarithmic terms partially cancel in the spectrum and completely cancel in the rate when the loop and tree graph contributions are added. Considering the fact that $(m_e/m_\mu)^2 = 2.34 \cdot 10^{-5}$, $(m_\mu/m_\tau)^2 = 3.54 \cdot 10^{-3}$ and $(m_e/m_\tau)^2 = 8.27 \cdot 10^{-8}$ the zero mass approximation should be a good approximation for most of the energy spectrum of the daughter leptons except for the region close (or very close) to the soft endpoint of the spectrum (also referred to as the threshold region) where finite mass effects have to be retained. In addition, when integrating the spectrum functions, the mass ratio enters linearly in all three polarized rate functions. Finite mass corrections may thus play an important role at least for $(\tau \rightarrow \mu)$ -decays where the linear mass ratio $m_\mu/m_\tau = 5.95 \cdot 10^{-2}$ is not very small. An improved analysis of τ -decays is of quite some topical interest since large samples of τ -leptons are currently being produced at the existing two B factories in Japan and in the USA and are expected to be produced at future τ -charm factories to be set up in Ithaca and Beijing.

We determine the radiative corrections to the daughter’s lepton energy spectrum and its longitudinal polarization keeping the dependence on the polarization of the parent lepton. This generalizes the calculation of [6] in which the zero mass approximation was used. Our calculation extends the calculation of [7], which also includes finite mass effects, in that we include the longitudinal polarization of the daughter lepton.

The paper is structured as follows. In Sec. 2 we introduce our notation and write down the general structure of the spin-dependent rate. Sec. 3 contains our Born term results. W -propagator effects are taken into account in Sec. 4. In Sec. 5 we present our analytical and numerical results on the radiative corrections. In Sec. 6 we consider the $m'_l \rightarrow 0$ limit of the $m'_l \neq 0$ results presented in Sec. 5 and discuss in some detail the origin of the anomalous helicity flip contribution. Sec. 7 contains our summary and conclusions. In two Appendices we collect some technical material on trilog functions and Fierz identities

¹The three leptonic μ - and τ -decays are treated within the Standard Model, i.e. they are all governed by the same $(V - A)$ coupling structure and coupling strength G_F .

relevant to our calculation.

2 General structure of spin-dependent rate

To make life simple we shall in the following always refer to the specific case $\mu^- \rightarrow e^- + \bar{\nu}_e + \nu_\mu$ instead of referring to the generic case involving also leptonic τ -decays when writing down analytical results. Of course, when discussing numerical results, the two leptonic τ -decay channels $\tau^- \rightarrow \mu^- + \bar{\nu}_\mu + \nu_\tau$ and $\tau^- \rightarrow e^- + \bar{\nu}_e + \nu_\tau$ are also included.

Since the subject of μ^- -decays is extensively covered in the relevant textbooks (see e.g. Refs. [8, 9, 10]) and review articles (see e.g. Refs. [11, 12, 13]) we can afford to be very brief in describing the formalism.

The spin-dependent differential rate for μ^- -decays is given by

$$\frac{d\Gamma}{dx d\cos\theta_P} = \beta x \Gamma_0 (G_1 + G_2 P \cos\theta_P + G_3 \cos\theta + G_4 P \cos\theta_P \cos\theta). \quad (1)$$

G_1 is the unpolarized spectrum function, G_2 and G_3 are single spin polarized spectrum functions referring to the spins of the μ^- and e^- , resp., and G_4 describes spin-spin correlations between the spin vectors of the μ^- and e^- . P denotes the degree of polarization of the decaying μ^- . As usual we introduce the scaled energy of the electron as $x = 2E_e/m_\mu$ where the energy is defined in the rest frame of the μ^- . The limits on x are given by $x_{min} = 2y$ and $x_{max} = 1 + y^2$ where $y = m_e/m_\mu$. We shall also make use of the velocity of the electron given by $\beta = \sqrt{1 - 4y^2/x^2}$. The polar angles θ_P and θ describe the orientation of the spins of the μ^- and e^- w.r.t. the momentum direction of the electron in the rest frame of the μ^- . One then has $\vec{\zeta}_\mu \vec{p}_e = p_e \cos\theta_P$ and $\vec{\zeta}_e \vec{p}_e = p_e \cos\theta$ where p_e is the magnitude of the three-momentum of the electron. $\vec{\zeta}_\mu$ and $\vec{\zeta}_e$ are the spin vectors of the μ^- and e^- in their respective rest frames. Γ_0 , finally, is the $m_e = 0$ Born term rate given by $\Gamma_0 = G_F^2 m_\mu^5 / 192\pi^3$. The differential rate for the charge conjugated decay $\mu^+ \rightarrow e^+ + \nu_e + \bar{\nu}_\mu$ is obtained from Eq. (1) by the substitution $G_2 \rightarrow -G_2$ and $G_4 \rightarrow -G_4$.

Note that the differential rate Eq. (1) contains only information on the projection of the spin vectors of the μ^- and e^- along the momentum direction of the electron. One thus calculates the longitudinal polarization of the electron. The dependence on transverse spin directions has dropped out because an azimuthal averaging about the electron direction is implied in the derivation of Eq. (1). If the azimuthal dependence of the differential rate is retained one will also have a dependence on the transverse spin component of the electron. Such azimuthal correlations will not be discussed in this paper.

It is convenient to split the unpolarized and polarized rate functions into a Born term part and a radiatively corrected part according to

$$G_i = G_i^{Born} + G_i^{(\alpha)} \quad i = 1, 2, 3, 4. \quad (2)$$

The respective results on the Born term contributions G_i^{Born} and the $O(\alpha)$ corrections to the rate functions $G_i^{(\alpha)}$ are given in Secs. 3 and 5.

3 Born term results

We shall work with the charge retention form of the Lagrangian for the decay $\mu^- \rightarrow e^- + \bar{\nu}_e + \nu_\mu$ which reads^{2,3}

$$\mathcal{L}(x) = \frac{G_F}{\sqrt{2}} \bar{\Psi}_e(x) \gamma^\alpha (\mathbb{1} - \gamma_5) \Psi_\mu(x) \bar{\Psi}_{\nu_\mu}(x) \gamma_\alpha (\mathbb{1} - \gamma_5) \Psi_{\nu_e}(x) + h.c. \quad (3)$$

When squaring the corresponding matrix element one obtains the tensor $C^{\alpha\beta}$ from the charged lepton side (C for charged) which has to be contracted with the neutrino-side tensor $N^{\alpha\beta}$ (N for neutral). For the Born term contribution of the charge-side tensor one obtains

$$C_{Born}^{\alpha\beta} = \frac{1}{4} \text{Tr} \left\{ (\not{p}_e + m_e) (\mathbb{1} + \gamma_5 \not{s}_e) \gamma^\alpha (\mathbb{1} - \gamma_5) (\not{p}_\mu + m_\mu) (\mathbb{1} + \gamma_5 \not{s}_\mu) \gamma^\beta (\mathbb{1} - \gamma_5) \right\}, \quad (4)$$

where the dependence on the polarization four-vectors of the μ^- and e^- has been retained.

Since only even-numbered γ -matrix strings survive between the two $(\mathbb{1} - \gamma_5)$ -factors in Eq. (4) one can compactly write the result of the trace evaluation as

$$C_{Born}^{\alpha\beta} = 2(\bar{p}_\mu^\beta \bar{p}_e^\alpha + \bar{p}_\mu^\alpha \bar{p}_e^\beta - g^{\alpha\beta} \bar{p}_\mu \cdot \bar{p}_e + i\epsilon^{\alpha\beta\gamma\delta} \bar{p}_{e,\gamma} \bar{p}_{\mu,\delta}), \quad (5)$$

where

$$\bar{p}_\mu^\alpha = p_\mu^\alpha - m_\mu s_\mu^\alpha, \quad (6)$$

$$\bar{p}_e^\alpha = p_e^\alpha - m_e s_e^\alpha \quad (7)$$

² The charge retention form of the Lagrangian is obtained from the usual Standard Model charged current-current form through the Fierz transformation (B1) written down in Appendix B. The minus sign from the Fierz identity is cancelled from having to commute the Fermion fields an odd number of times in order to relate the two forms. Note that the Fierz identity is a four-dimensional identity. Since our calculations are done in four dimensions the Fierz identity can be safely applied.

³When the Lagrangian for μ -decay is written in charge retention form the similarity of the decay $\mu^- \rightarrow e^- + \bar{\nu}_e + \nu_\mu$ to the decay $b \rightarrow c + e^- + \bar{\nu}_e$ becomes quite apparent through the substitutions $b \leftrightarrow \mu^-$, $c \leftrightarrow e^-$, $e^- \leftrightarrow \nu_\mu$ and $\bar{\nu}_e \leftrightarrow \bar{\nu}_e$.

and where s_μ^α and s_e^α are the polarization four-vectors of the μ^- and e^- , respectively. In the μ^- rest system they read

$$s_\mu^\alpha = (0; \vec{\zeta}_\mu), \quad (8)$$

$$s_e^\alpha = \left(\frac{\vec{\zeta}_e \vec{p}_e}{m_e}; \vec{\zeta}_e + \frac{\vec{\zeta}_e \vec{p}_e}{m_e(E_e + m_e)} \vec{p}_e \right). \quad (9)$$

The dependence on the momentum directions of the $\bar{\nu}_e$ - and ν_μ -neutrinos has been completely integrated out in the differential rate. Thus the neutrino-side of the interaction can only depend on the spatial piece of the second rank tensor build from the momentum transfer to the neutrinos (for the present purpose the neutrinos are treated as massless) which we denote by Q^α ⁴. Thus the relevant neutrino-side tensor is given by

$$N^{\alpha\beta} = -g^{\alpha\beta} + \frac{Q^\alpha Q^\beta}{Q^2}. \quad (10)$$

The Born spectrum functions can then be extracted from

$$Q^2 N^{\alpha\beta} C_{\alpha\beta}^{Born} = 2((\vec{p}_\mu \cdot \vec{p}_e) Q^2 + 2(\vec{p}_\mu \cdot Q)(\vec{p}_e \cdot Q)), \quad (11)$$

where the antisymmetric piece in $C_{\alpha\beta}^{Born}$ has dropped out after the symmetric contraction. At the Born term level one has $Q = p_\mu - p_e$.

The scalar products in Eq. (11) are best evaluated in the rest system of the μ^- . Including the correct normalization the differential Born term rate is given by

$$\frac{d\Gamma^{Born}}{dx d\cos\theta_P} = \Gamma_0 \beta x \frac{Q^2 N^{\alpha\beta} C_{\alpha\beta}^{Born}}{m_\mu^4}. \quad (12)$$

The spectrum functions defined in Eq. (1) can then easily be read off from the Born term contributions (11). They are given by

$$\begin{aligned} G_1^{Born} &= (3 - 2x)x - (4 - 3x)y^2, \\ G_2^{Born} &= \beta x(1 - 2x + 3y^2), \\ G_3^{Born} &= -\beta x(3 - 2x + y^2), \\ G_4^{Born} &= -(1 - 2x)x - (4 + x)y^2. \end{aligned} \quad (13)$$

⁴We denote the momentum transfer to the neutrino pair by a capital Q in order to set it apart from the momentum transfer q to the $(e^- \bar{\nu}_e)$ -pair used in Sec. 4.

Note that the Born term spectrum functions are quadratically dependent on y^2 . For $y^2 = 0$ ($m_e = 0$) the Born term results (13) reproduce the results of Ref. [6]. For $y^2 \neq 0$ ($m_e \neq 0$) our Born term results for G_1^{Born} and G_2^{Born} agree with those of Ref. [7].

In Figs. 1a ($\mu \rightarrow e$), 2a ($\tau \rightarrow \mu$) and 3a ($\tau \rightarrow e$) we show plots of the x -dependence of the four Born term spectrum functions $\beta x G_i^{Born}$. They rise from zero at the soft end of the spectrum to $(1 - y^2)^3$ ($i = 1, 4$) and $-(1 - y^2)^3$ ($i = 2, 3$) at the hard end of the spectrum. The $m_\nu = 0$ pattern $G_1(x) = -G_3(x)$ and $G_2(x) = -G_4(x)$ is slightly distorted by final state mass effects except for the point $x_{max} = 1 + y^2$ where the above relations are exact.

The longitudinal polarization P_e^l of the electron is defined by

$$P_e^l = \frac{d\Gamma(\cos\theta = 1) - d\Gamma(\cos\theta = -1)}{d\Gamma(\cos\theta = 1) + d\Gamma(\cos\theta = -1)}. \quad (14)$$

Similarly the forward-backward asymmetry A_{FB} is given by

$$A_{FB} = \frac{d\Gamma(0 \leq \theta_P \leq \pi/2) - d\Gamma(\pi/2 \leq \theta_P \leq \pi)}{d\Gamma(0 \leq \theta_P \leq \pi/2) + d\Gamma(\pi/2 \leq \theta_P \leq \pi)}. \quad (15)$$

In terms of the spectrum functions defined in Eq. (1) one obtains

$$P_e^l = \frac{G_3 + G_4 P \cos\theta_P}{G_1 + G_2 P \cos\theta_P} \quad (16)$$

and

$$A_{FB} = P \frac{G_2 + G_4 \cos\theta}{G_1 + G_3 \cos\theta}. \quad (17)$$

Inserting the Born spectrum functions from (13) one finds

$$P_e^l(x) = -\frac{\beta x(3 - 2x + y^2) + ((1 - 2x)x + (4 + x)y^2) P \cos\theta_P}{(3 - 2x)x - (4 - 3x)y^2 + \beta x(1 - 2x + 3y^2) P \cos\theta_P} \quad (18)$$

and

$$A_{FB} = P \frac{\beta x(1 - 2x + 3y^2) - ((1 - 2x)x + (4 + x)y^2) \cos\theta}{(3 - 2x)x - (4 - 3x)y^2 - \beta x(3 - 2x + y^2) \cos\theta}. \quad (19)$$

The longitudinal polarization and the forward-backward asymmetry take the values $P_e^l = -\frac{1}{3}P \cos\theta_P$ and $A_{FB} = -\frac{1}{3}P \cos\theta$, respectively, at the lower limit $x_{min} = 2y$ where $G_1^{Born} = -3G_4^{Born}$ and $G_2^{Born} = G_3^{Born} = 0$. At the upper limit $x_{max} = (1 + y^2)$, where $G_1^{Born} = -G_2^{Born} = -G_3^{Born} = G_4^{Born} = (1 - y^2)^2$, the longitudinal polarization and the

	$\mu \rightarrow e$		$\tau \rightarrow \mu$		$\tau \rightarrow e$	
	Born	(α)	Born	(α)	Born	(α)
\hat{G}_1	-0.019%	-0.12%	-2.82%	- 8.48%	$-6.62 \cdot 10^{-5}\%$	$-7.39 \cdot 10^{-4}\%$
\hat{G}_2	$-3.57 \cdot 10^{-4}\%$	-0.67%	-0.57%	-11.23%	$-7.60 \cdot 10^{-8}\%$	-0.039%
\hat{G}_3	-0.031%	-1.48%	-4.25%	-24.49%	$-1.10 \cdot 10^{-4}\%$	-0.084%
\hat{G}_4	-0.019%	-1.43%	-2.82%	-22.15%	$-6.62 \cdot 10^{-5}\%$	-0.083%

Table 1:

Percentage mass corrections to $m_\nu = 0$ (Born) and $m_\nu \rightarrow 0$ ($O(\alpha)$) rate functions for the three cases $\mu \rightarrow e$, $\tau \rightarrow \mu$ and $\tau \rightarrow e$.

forward-backward asymmetry decrease to $P_e^l = -1$ irrespective of the value of $P \cos \theta_P$ and to $A_{FB} = -P$ irrespective of the value of $\cos \theta$. This has to be contrasted with the naive limit $P_e^l = -1$ and $A_{FB} = P(1-2x)/(3-2x)$ when naively setting $y = 0$ in Eqs. (18) and (19).

In Figs. 1b ($\mu \rightarrow e$), 2b ($\tau \rightarrow \mu$) and 3b ($\tau \rightarrow e$) we show the x dependence of the Born term prediction for the longitudinal polarization of the daughter lepton for the three values $\cos \theta_P = 1, 0$ and -1 and $P = 1$. The longitudinal polarization stays close to -1 over most of the (hard part) of the spectrum but deviates significantly from the naive value -1 in the threshold region with only a slight dependence on the value of $\cos \theta_P$. In order to highlight the deviation from the naive value $P_e^l = -1$ in the threshold region we have chosen logarithmic scales for the energy variable x . The three Born term curves can be seen to approach the limits discussed above at the soft and hard end of the spectrum.

In Figs. 1c, 2c and 3c we show the corresponding curves for the forward-backward asymmetry A_{FB} for the three decay cases. The forward-backward asymmetries rise from the limiting value $A_{FB} = -1$ at the hard end of the spectrum to $A_{FB} = -1/3 P \cos \theta$ at threshold. Contrary to naive expectations there is a strong $\cos \theta$ dependence for $\cos \theta$ values close to 1, i.e. for helicities of the daughter leptons close to $\lambda_\nu = 1/2$. This is due to the fact that the leading terms in the small y expansion tend to cancel in the numerator and denominator of the asymmetry ratio close to $\cos \theta = 1$ (the leading terms cancel exactly for $\cos \theta = 1$ since the massless electron emerging from the weak ($V - A$) vertex is left-handed).

Next we integrate the differential Born term rates over the full x spectrum. Let us define reduced Born rate functions \hat{G}_i^{Born} according to

$$\hat{G}_i^{Born} = \int_{2y}^{1+y^2} dx \beta x G_i^{Born} \quad i = 1, 2, 3, 4. \quad (20)$$

One obtains

$$\begin{aligned} \hat{G}_1^{Born} &= \frac{1}{2}(1 - y^4)(1 - 8y^2 + y^4) - 12y^4 \ln y = \frac{1}{2} - 4y^2 + O(y^4), \\ \hat{G}_2^{Born} &= -\frac{1}{6}(1 - y)^5(1 + 5y + 15y^2 + 3y^3) = -\frac{1}{6} + \frac{16}{3}y^3 + O(y^4), \\ \hat{G}_3^{Born} &= -\frac{1}{6}(1 - y)^5(3 + 15y + 5y^2 + y^3) = -\frac{1}{2} + \frac{20}{3}y^2 - 16y^3 + O(y^4), \\ \hat{G}_4^{Born} &= \frac{1}{6}(1 - y^4)(1 - 8y^2 + y^4) - 4y^4 \ln y = \frac{1}{6} - \frac{4}{3}y^2 + O(y^4). \end{aligned} \quad (21)$$

The occurrence of odd powers of y in \hat{G}_2^{Born} and \hat{G}_3^{Born} can be traced to the lower boundary $x = 2y$ of the x -integration which is linear in y . In view of this it is quite remarkable that \hat{G}_1^{Born} and \hat{G}_4^{Born} contain only even powers of y . Nevertheless, the leading mass correction to \hat{G}_3^{Born} sets in only at $O(y^2)$ and, for \hat{G}_2^{Born} , only at $O(y^3)$. In this sense the Born term rates are well protected against finite electron mass effects, or, in the case ($\tau \rightarrow \mu$), reasonably well against muon mass effects. This is illustrated in Table 1 where we list the values of the Born term percentage changes $(\hat{G}_i(m \neq 0) - \hat{G}_i(m = 0))/\hat{G}_i(m = 0)$ when going from $m_\nu = 0$ to $m_\nu \neq 0$ for all three cases.

The average longitudinal polarization of the electron $\langle P_e^l \rangle$ and the average forward-backward asymmetry $\langle A_{FB} \rangle$ is obtained by the replacement ($G_i \rightarrow \hat{G}_i$) in (16) and (17). As in the rate expressions (21) the electron mass effect on the Born term polarization $\langle P_e^l \rangle$ is quite small. The deviation from the $m_\nu = 0$ result $\langle P_\nu^l \rangle = -1$ is of $O(10^{-4})$ in muon decay and $O(10^{-6})$ in ($\tau \rightarrow e$). For ($\tau \rightarrow \mu$) the deviation from $\langle P_\mu^l \rangle = -1$ is of $O(10^{-2})$. The dependence on the value of $P \cos \theta_P$ is very small. The average values of the forward-backward asymmetry $\langle A_{FB} \rangle$ are quite close ($O(10^{-2} - 10^{-3})$) to the $y = 0$ prediction $\langle A_{FB} \rangle = -1/3$ except for the case $\tau \rightarrow \mu$ and $\cos \theta = 1$ where one finds $\langle A_{FB} \rangle = -0.536$. The case $\cos \theta = 1$ is in fact special and will be discussed further at the end of Sec. 5.

4 W -boson propagator effects

In order to incorporate W -boson propagator effects one has to rewrite the charge retention form of the four-Fermi interaction (3) in terms of the charged currents of the

Standard Model including the W -boson propagator. This is easily done using the Fierz transformation property written down in Eq. (B1) in Appendix B.

For the present purposes it is only necessary to take into account W -boson propagator effects in the Born term. The momentum transfer is now $q = p_\mu - p_{\nu_\mu} = p_e + p_{\nu_e}$. The $q^\mu q^\nu$ piece of the W -boson propagator contributes only at $O(m_e m_\mu / m_W^2)$ and can therefore be dropped. In fact, using the Fierz identity (B2), it is not difficult to compute the contribution of the $q^\mu q^\nu$ piece exactly. The W -boson propagator effect on the spectrum can thus be taken into account by the replacement

$$1 \rightarrow \left(\frac{m_W^2}{q^2 - m_W^2} \right)^2 \approx 1 + 2 \frac{m_\mu^2}{m_W^2} (1 - x), \quad (22)$$

where terms of $O(m_e^2/m_W^2)$ have been neglected. Numerically the propagator corrections are quite small since $m_\mu^2/m_W^2 = 1.73 \cdot 10^{-6}$ and $m_\tau^2/m_W^2 = 4.88 \cdot 10^{-4}$.

It is evident that inclusion of W -boson propagator effects does not affect the energy dependence of the longitudinal polarization of the electron or the forward-backward asymmetry since the correction factor in Eq. (22) drops out in the ratios Eqs. (16) and (17).

In order to determine the propagator corrections to the rate functions one has to do the integrations

$$\int_0^1 dx x G_{1,3}^{Born} \left(1 + 2 \frac{m_\mu^2}{m_W^2} (1 - x) \right) = \pm \frac{1}{2} \left(1 + \frac{3}{5} \frac{m_\mu^2}{m_W^2} \right), \quad (23)$$

$$\int_0^1 dx x G_{2,4}^{Born} \left(1 + 2 \frac{m_\mu^2}{m_W^2} (1 - x) \right) = \mp \frac{1}{6} \left(1 + \frac{1}{5} \frac{m_\mu^2}{m_W^2} \right), \quad (24)$$

where terms of $O(y)$ have been dropped in the Born term factors and in the integration measure. As is evident from Eq. (23) and Eq. (24) the W -boson propagator affects the two pairs of rate functions differently. This means that one cannot absorb the W -boson propagator effect entirely into a redefinition of Fermi's coupling constant G_F , as recently advocated in Refs. [14, 15], if one is considering spectrum averaged polarization effects. If the W -boson propagator effect is absorbed into a redefinition of G_F using a measurement of the total unpolarized rate then this must be compensated for by multiplying the polarization dependent pieces $\hat{G}_{2,4}$ by $(1 - \frac{2}{5} \frac{m_\mu^2}{m_W^2})$ when calculating the average of the longitudinal polarization of the electron $\langle P_e^l \rangle$ or the forward-backward asymmetry $\langle A_{FB} \rangle$.

5 $O(\alpha)$ corrections to spin dependent rate functions

Many of the technical ingredients that go into the calculation of the $O(\alpha)$ corrections can be found in a detailed account of the $O(\alpha_s)$ corrections to the decay of a polarized top into a bottom quark and a W gauge boson $t \rightarrow b + W^+$ presented in Ref. [2] (for the loop contribution see also [16]). Compared to Ref. [2] one needs to include the polarization dependence of the final massive fermion in this application. For the $O(\alpha)$ tree-graph and one-loop contributions this is easily done.

Let us briefly discuss the tree graph contribution. The $O(e)$ tree graph amplitude (“internal bremsstrahlung”) consists of the two contributions where the photon is either radiated off the muon or off the electron. One thus has

$$\mathcal{M}^\alpha = e \bar{u}_e \left(\gamma^\delta \frac{\not{p}_e + \not{k} + m_e}{(p_e + k)^2 - m_e^2} \gamma^\alpha (\mathbb{1} - \gamma_5) + \gamma^\alpha (\mathbb{1} - \gamma_5) \frac{\not{p}_\mu - \not{k} + m_\mu}{(p_\mu - k)^2 - m_\mu^2} \gamma^\delta \right) u_\mu \epsilon_\delta^*, \quad (25)$$

where k and ϵ_δ are the momentum and the polarization four-vector of the photon. Four-momentum conservation now reads $p_\mu = p_e + Q + k$ where Q is again the momentum transferred to the neutrino pair. When squaring the tree graph amplitude one only sums over the polarization states of the photon since the muon and the electron are taken as polarized. Omitting again the antisymmetric contribution one obtains

$$\begin{aligned} C^{(\alpha)\alpha\beta} &= \sum_{\gamma\text{-spin}} \mathcal{M}^\alpha \mathcal{M}^{\beta\dagger} = \frac{e^2}{2} \left\{ \frac{1}{(k \cdot p_e)} \left(\frac{k \cdot \bar{p}_e - m_e^2}{(k \cdot p_e)} + \frac{p_\mu \cdot \bar{p}_e}{(k \cdot p_\mu)} \right) (k^\alpha \bar{p}_\mu^\beta + k^\beta \bar{p}_\mu^\alpha - k \cdot \bar{p}_\mu g^{\alpha\beta}) \right. \\ &+ \frac{1}{(k \cdot p_\mu)} \left(\frac{k \cdot \bar{p}_\mu + m_\mu^2}{(k \cdot p_\mu)} - \frac{p_e \cdot \bar{p}_\mu}{(k \cdot p_e)} \right) (k^\alpha \bar{p}_e^\beta + k^\beta \bar{p}_e^\alpha - k \cdot \bar{p}_e g^{\alpha\beta}) \\ &+ \frac{k \cdot \bar{p}_e}{(k \cdot p_e)^2} (p_e^\alpha \bar{p}_\mu^\beta + p_e^\beta \bar{p}_\mu^\alpha - p_e \cdot \bar{p}_\mu g^{\alpha\beta}) - \frac{k \cdot \bar{p}_\mu}{(k \cdot p_\mu)^2} (p_\mu^\alpha \bar{p}_e^\beta + p_\mu^\beta \bar{p}_e^\alpha - p_\mu \cdot \bar{p}_e g^{\alpha\beta}) \\ &+ \left. \frac{k \cdot \bar{p}_\mu}{(k \cdot p_e)(k \cdot p_\mu)} (p_e^\alpha \bar{p}_e^\beta + p_e^\beta \bar{p}_e^\alpha - m_e^2 g^{\alpha\beta}) - \frac{k \cdot \bar{p}_e}{(k \cdot p_e)(k \cdot p_\mu)} (p_\mu^\alpha \bar{p}_\mu^\beta + p_\mu^\beta \bar{p}_\mu^\alpha - m_\mu^2 g^{\alpha\beta}) \right\} \\ &- \frac{e^2}{2} \left(\bar{p}_e^\alpha \bar{p}_\mu^\beta + \bar{p}_e^\beta \bar{p}_\mu^\alpha - \bar{p}_e \cdot \bar{p}_\mu g^{\alpha\beta} \right) \left(\frac{m_\mu^2}{(k \cdot p_\mu)^2} + \frac{m_e^2}{(k \cdot p_e)^2} - 2 \frac{p_e \cdot p_\mu}{(k \cdot p_e)(k \cdot p_\mu)} \right). \quad (26) \end{aligned}$$

In the last line of Eq. (26) we have isolated the infrared singular piece of the charge-side tensor which is given by the usual soft photon factor multiplying the Born term

contribution. In the phase space integration over the photon momentum the infrared singular piece is regularized by introducing a (small) photon mass the contribution of which is cancelled by the corresponding one-loop contributions. The remaining part of the charge-side tensor is infrared finite and can easily be integrated.

Just as in the Born term case treated in Sec. 3 the $O(\alpha)$ charge-side tensor $C_{\alpha\beta}^{(\alpha)}$ is contracted with the neutral-side tensor $N^{\alpha\beta}$ Eq. (10) where now $Q = p_\mu - p_e - k$. One then performs the appropriate tree graph integrations over the photon's momentum and adds in the one-loop contributions. The final result is

$$\begin{aligned}
G_1^{(\alpha)} &= \frac{\alpha}{\pi} G_1^{Born} \Sigma + \frac{\alpha}{\pi} \frac{1}{12\beta x} \left\{ 3\beta x \left((3-4x)x - (8-9x)y^2 \right) \lambda_1 \right. \\
&\quad + \left((5+12x-51x^2+28x^3) - 3(19-40x+17x^2)y^2 - 3(19-4x)y^4 + 5y^6 \right) \lambda_2 \\
&\quad \left. - 4\beta x \left((11-10x+5x^2) - 2(1+5x)y^2 + 11y^4 \right) \right\}, \tag{27}
\end{aligned}$$

$$\begin{aligned}
G_2^{(\alpha)} &= \frac{\alpha}{\pi} G_2^{Born} \Sigma + \frac{\alpha}{\pi} \frac{1}{12\beta^2 x^2} \left\{ 3\beta^3 x^3 (1-4x+9y^2) \lambda_1 - 8(1-x+y^2)^3 \lambda_3 \right. \\
&\quad - \left(x(1+33x^2-28x^3) - 3x(33-12x-17x^2)y^2 + 3(32-35x-4x^2)y^4 - 5xy^6 \right) \lambda_2 \\
&\quad \left. - 2\beta x \left((3-10x-13x^2+8x^3) + (59-11x^2)y^2 - (35-10x)y^4 + 5y^6 \right) \right\}, \tag{28}
\end{aligned}$$

$$\begin{aligned}
G_3^{(\alpha)} &= \frac{\alpha}{\pi} G_3^{Born} \Sigma + \frac{\alpha}{\pi} \frac{1}{12\beta^2 x^2} \left\{ -3\beta^3 x^3 (3-4x+3y^2) \lambda_1 - 8y^2 (1-x+y^2)^3 \lambda_3 \right. \\
&\quad - \left(x(5+12x-51x^2+28x^3) - (8-129x+60x^2+25x^3)y^2 \right. \\
&\quad \left. - 3(40-49x+8x^2)y^4 - (24-23x)y^6 - 8y^8 \right) \lambda_2 \\
&\quad \left. + 2\beta x \left((5+10x-11x^2+8x^3) - (35+13x^2)y^2 + (59-10x)y^4 + 3y^6 \right) \right\}, \tag{29}
\end{aligned}$$

$$\begin{aligned}
G_4^{(\alpha)} &= \frac{\alpha}{\pi} G_4^{Born} \Sigma + \frac{\alpha}{\pi} \frac{1}{12\beta^3 x^3} \left\{ -3\beta^3 x^3 \left((1-4x)x + (8+3x)y^2 \right) \lambda_1 \right. \\
&\quad \left. + 8x(1-y^2)(1-x+y^2)^3 \lambda_3 + 4\beta x \left(x(1-5x-5x^2+3x^3) \right) \right\}
\end{aligned}$$

$$\begin{aligned}
& - (4 - 59x + 14x^2 + 5x^3)y^2 - (104 - 59x + 5x^2)y^4 - (4 - x)y^6) \\
& + \left(x^2(1 + 33x^2 - 28x^3) + (4 + 8x - 153x^2 + 104x^3 + 25x^4)y^2 \right. \\
& \left. - 3(28 - 72x + 59x^2 - 8x^3)y^4 - (84 - 24x + 23x^2)y^6 + 4(1 + 2x)y^8 \right) \lambda_2 \Big\}. \quad (30)
\end{aligned}$$

We have used the abbreviations

$$\lambda_1 = \ln y^2, \quad \lambda_2 = \ln \left(\frac{1 + \beta}{1 - \beta} \right), \quad \lambda_3 = \ln \left(\frac{2 - (1 + \beta)x}{2 - (1 - \beta)x} \right) \quad (31)$$

and

$$\begin{aligned}
\Sigma &= \frac{1}{\beta} \left\{ 2\text{Li}_2 \left(\frac{2\beta x}{2 - (1 - \beta)x} \right) - 2\text{Li}_2 \left(\frac{2\beta x}{(1 + \beta)x - 2y^2} \right) - \beta \ln(1 - x + y^2) \right. \\
&\left. + \left(\ln \left((1 + \beta) \frac{x}{2} \right) - \frac{1 - y^2}{x} \right) (\lambda_3 - \lambda_2) + \left(\ln \left(1 - (1 + \beta) \frac{x}{2} \right) - \frac{1 - x}{x} \right) \lambda_2 \right\}. \quad (32)
\end{aligned}$$

Our results for G_1 and G_2 agree with those of [7]. Note that that all four spectrum functions are logarithmically mass divergent. We have checked that the expansion of the spectrum functions in terms of powers of y contains only even powers of y , in agreement with the general reasoning presented in [17]. The leading term in this expansion can be reconstructed from the $m_e \rightarrow 0$ results listed in Sec. 6. We have not listed the higher order coefficients since they are not particularly illuminating.

In Fig. 1a ($\mu \rightarrow e$), Fig. 2a ($\tau \rightarrow \mu$) and Fig. 3a ($\tau \rightarrow e$) we show plots of the x dependence of the four spectrum functions $\beta x G_i$, with and without radiative corrections. The radiative corrections show a marked y dependence. They are smallest for $\tau \rightarrow \mu$, become larger for $\mu \rightarrow e$, and are largest for $\tau \rightarrow e$. To a large part this can be traced back to the $\ln y$ dependent terms in the spectrum functions. On an *absolute* scale the radiative corrections are generally quite small except for the hard end of the spectrum where they in fact diverge. The divergent behaviour at the hard end of the spectrum will be discussed later on. On a *relative* scale the radiative corrections are quite large for ($\mu \rightarrow e$) and for ($\tau \rightarrow e$), and smaller for ($\tau \rightarrow \mu$) at the soft end of the spectrum, where the spectrum functions are small. This will show up in the radiative corrections to the longitudinal polarization of daughter lepton P_i^l and the forward-backward asymmetry

A_{FB} which are large in the threshold region for $\mu \rightarrow e$ and $\tau \rightarrow e$ and quite moderate for $\tau \rightarrow \mu$.

It is interesting to note that the radiative corrections go through zeros close to $x = 0.68$ and $x = 0.82$ for $G_{1,3}$ and for $G_{2,4}$, respectively, for all three cases discussed in this paper. The positions of the respective zeros are practically mass independent. Differences in the position of the zero show up only in the third digit. In fact, when discussing the $m_\mu \rightarrow 0$ case in Sec. 6 we have checked that the positions of the zeroes remain practically unchanged even when letting $y \rightarrow 0$. The radiative corrections are negative and positive below and above the zero for $\beta x G_{1,4}$, resp., and positive and negative below and above the zero for $\beta x G_{2,3}$. Qualitatively the alternating sign pattern can be understood from the dominance of the $\ln y$ terms and from the fact that the $\ln y$ dependent terms have to cancel out when one integrates over the spectrum. There is a tendency of the radiative corrections to cancel in the sums $(G_1 + G_3)$ and $(G_2 + G_4)$ and to add up in the differences $(G_1 - G_3)$ and $(G_2 - G_4)$, i.e. the radiative corrections add destructively and constructively in the final electron's density matrix elements ρ_{++} and ρ_{--} , resp., to be discussed further in Sec. 6.

We next turn to the radiative corrections of the longitudinal polarization of the daughter lepton P'_l and the forward-backward asymmetry A_{FB} calculated according to Eqs. (16) and (17). We begin by discussing the limiting value of the longitudinal polarization at the soft end of the spectrum including the radiative corrections. One has

$$\begin{aligned} \lim_{x \rightarrow 2y} P_e^l &= -\frac{1}{3} P \cos \theta_P \left\{ 1 - \frac{\alpha}{\pi} \frac{4(1-y)^2(1+y^2)}{72y^2 + \frac{\alpha}{\pi}(5-10y-278y^2-10y^3+5y^4) - 108 \frac{1+y}{1-y} y^2 \ln y} \right\} \\ &\approx -\frac{1}{3} P \cos \theta_P \left\{ 1 - \frac{\alpha}{\pi} \left(18y^2 + \frac{5}{4} \frac{\alpha}{\pi} \right)^{-1} \right\}. \end{aligned} \quad (33)$$

For the cases $\mu \rightarrow e$ and $\tau \rightarrow e$ the term $18y^2$ in the second line of (33) can be neglected and thus the limiting value of the longitudinal polarization of the electron is given by $P_e^l \approx -\frac{1}{15} P \cos \theta_P$ which is smaller than the Born term value by a factor of 5. This is evident in Figs. 1b and 3b where the radiative corrections to the longitudinal polarization of the electron are shown. For the $\tau \rightarrow \mu$ case the term $18y^2$ dominates over $(5/4)(\alpha/\pi)$ and the limiting value of the longitudinal polarization of the μ is $P_e^l \approx -\frac{1}{3} P \cos \theta_P (1 - \frac{\alpha}{\pi} \frac{1}{18y^2})$, i.e. the correction to the Born term value is only $\approx 3.6\%$. This is again seen in Fig. 2b. The limiting values for the forward-backward asymmetries follow the same pattern since the spectral functions $\beta x G_1$ and $\beta x G_4$ are dominant at threshold. This can again be seen in Figs. 1c - 3c.

Next we discuss the limiting behaviour of the spectrum functions at the hard end of the spectrum, where $x \rightarrow x_{max} = 1 + y^2$. The radiative correction contributions can be seen to logarithmically diverge in this limit⁵. Introducing $x'_{max} = 1 + y^2 - \varepsilon$ the limiting behaviour of the four spectrum functions can be seen to be given by

$$\lim_{x \rightarrow x_{max}} G_1 = - \lim_{x \rightarrow x_{max}} G_2 = - \lim_{x \rightarrow x_{max}} G_3 = \lim_{x \rightarrow x_{max}} G_4 = (1 - y^2)^2 + \frac{\alpha}{\pi} 2(1 - y^2) \times \quad (34)$$

$$\times \left\{ (1 + y^2) \left(\frac{3}{4} + \ln \left(\frac{\varepsilon}{1 - y^2} \right) \right) \ln y + (1 - y^2) \left(1 + \ln \left(\frac{\varepsilon}{1 - y^2} \right) \right) \right\}.$$

The limiting values of the four spectrum functions are seen to be, up to signs, all identical. This implies that the radiative corrections to the longitudinal polarization of the daughter lepton does not change the Born term value $P_{l'}^l = -1$ at the hard end of the spectrum irrespective of the values of $P \cos \theta_P$. Similarly the radiative corrections to the forward-backward asymmetry do not change the Born term value of $A_{FB} = -P$ at the hard end of the spectrum irrespective of the value of $\cos \theta$.

The fact that the corrections to the spectrum functions in the threshold region are *relatively* large for $(\mu \rightarrow e)$ and $(\tau \rightarrow e)$ shows up in Figs. 1b and 3b, and in Figs. 1c and 3c, where the radiative corrections to the longitudinal polarization of the final state electrons and the forward-backward asymmetry are visibly large in the threshold region⁶. Note, though, that we have enhanced the threshold region in our presentation of P_e^l and A_{FB} by choosing a logarithmic scale for x in Figs. 1b,c, 2b,c and 3b,c. For the forward-backward asymmetry the radiative corrections remain large over a larger part of the spectrum. In particular for $\cos \theta = 1$ the radiative corrections to A_{FB} are significant over almost the complete spectrum. The radiative corrections to P_e^l and A_{FB} for the $(\tau \rightarrow \mu)$ decays are shown in Figs. 2b and 2c. As expected from the smallness of the radiative corrections to the rate functions shown in Fig. 2a the radiative corrections to both the longitudinal polarization of the final state muon and the forward-backward asymmetry are small. Since the rate functions are small at the soft end of the spectrum, the radiatively corrected average longitudinal polarization $\langle P_{l'}^l \rangle$ of the daughter lepton l' is expected to remain very close to -1 in all three cases. Using the integrated rate functions presented at the end of this section we find $\langle P_{l'}^l \rangle = -0.999, -0.986$ and -0.999 for $(\mu \rightarrow e), (\tau \rightarrow \mu)$

⁵The divergent terms at the endpoint of the electron spectrum can be resummed and converted into an exponential function [18, 19].

⁶In our numerical results for the longitudinal polarization of the final state daughter lepton and the forward-backward asymmetry we have not expanded out the inverse of the denominator function in terms of powers of α .

and ($\tau \rightarrow e$), resp., with very little dependence on $\cos \theta_P$. The corresponding figures for A_{FB} are $(-0.333, -0.333, -0.352)$, $(-0.339, -0.340, -0.536)$ and $(-0.332, -0.332, -0.334)$ for $P = 1$ and $\cos \theta = -1, 0, 1$.

Next we integrate the four spectrum functions $\beta x G_i^{(\alpha)}$ over the electron spectrum according to (20). One obtains

$$\begin{aligned}
\hat{G}_1^{(\alpha)} = & \frac{\alpha}{\pi} \left\{ \frac{1}{48} (1 - y^4) (75 - 956y^2 + 75y^4) - y^4 (36 + y^4) \ln^2 y \right. \\
& - \frac{\pi^2}{4} (1 - 32y^3 + 16y^4 - 32y^5 + y^8) - \frac{1}{6} (60 + 270y^2 - 4y^4 + 17y^6) y^2 \ln y \\
& - \frac{1}{12} (1 - y^4) (17 - 64y^2 + 17y^4) \ln(1 - y^2) \\
& + 2(1 - y)^4 (1 + 4y + 10y^2 + 4y^3 + y^4) \ln(1 - y) \ln y \\
& + 2(1 + y)^4 (1 - 4y + 10y^2 - 4y^3 + y^4) \ln(1 + y) \ln y \\
& + (3 + 32y^3 + 48y^4 + 32y^5 + 3y^8) \text{Li}_2(-y) \\
& \left. + (3 - 32y^3 + 48y^4 - 32y^5 + 3y^8) \text{Li}_2(y) \right\}, \tag{35}
\end{aligned}$$

$$\begin{aligned}
\hat{G}_2^{(\alpha)} = & \frac{\alpha}{\pi} \left\{ \frac{1}{3} (1 - y^2) (1 + y^2 + 13y^4 - 3y^6) (\ln(1 - y) + 2 \ln(1 + y)) \ln y \right. \\
& - \frac{1}{432} (1 - y)^2 (617 - 842y + 1929y^2 - 1592y^3 - 3415y^4 + 54y^5 - 567y^6) \\
& - \frac{1}{36} (1 - y) y (12 - 18y - 238y^2 + 41y^3 - 1003y^4 - 45y^5 - 9y^6) \ln y \\
& + \frac{1}{36} (1 - y)^2 (13 + 26y + 87y^2 - 364y^3 + 535y^4 - 102y^5 - 51y^6) \ln(1 - y) \\
& + \frac{1}{2} y^4 (14 + 32y^2 - 3y^4) \ln^2 y - \frac{1}{9} (1 - y^2) (25 + 13y^2 + 67y^4 + 15y^6) \ln(1 + y) \\
& \left. - 8y^4 \left(\frac{1}{6} \ln^3 y + \left(2\text{Li}_2(-y) + \text{Li}_2(y) - \frac{\pi^2}{3} \right) \ln y - 6\text{Li}_3(-y) - \text{Li}_3(y) - \frac{7}{2} \zeta(3) \right) \right\}
\end{aligned}$$

$$+ \frac{1}{3}(7 + 24y^2 + 48y^4 - 8y^6 + 9y^8) \left(\text{Li}_2(-y) + \frac{\pi^2}{12} \right), \quad (36)$$

$$\begin{aligned} \hat{G}_3^{(\alpha)} &= \frac{\alpha}{\pi} \left\{ \frac{1}{3}(1 - y^2)(3 - 13y^2 - y^4 - y^6)(\ln(1 - y) + 2 \ln(1 + y)) \ln y \right. \\ &\quad - \frac{1}{432}(1 - y)^2(567 - 54y + 3415y^2 + 1592y^3 - 1929y^4 + 842y^5 - 617y^6) \\ &\quad - \frac{1}{36}(1 - y)y(36 + 98y + 590y^2 - 265y^3 + 27y^4 - 99y^5 - 87y^6) \ln y \\ &\quad + \frac{1}{36}(1 - y)^2(51 + 102y - 535y^2 + 364y^3 - 87y^4 - 26y^5 - 13y^6) \ln(1 - y) \\ &\quad - \frac{1}{6}y^2(8 + 66y^2 - 24y^4 - y^6) \ln^2 y - \frac{1}{9}(1 - y^2)(15 + 67y^2 + 13y^4 + 25y^6) \ln(1 + y) \\ &\quad + 8y^4 \left(\frac{1}{6} \ln^3 y + \left(2\text{Li}_2(-y) + \text{Li}_2(y) - \frac{\pi^2}{3} \right) \ln y - 6\text{Li}_3(-y) - \text{Li}_3(y) - \frac{7}{2}\zeta(3) \right) \\ &\quad \left. + \frac{1}{3}(9 - 8y^2 + 48y^4 + 24y^6 + 7y^8) \left(\text{Li}_2(-y) + \frac{\pi^2}{12} \right) \right\}, \quad (37) \end{aligned}$$

$$\begin{aligned} \hat{G}_4^{(\alpha)} &= \frac{\alpha}{\pi} \left\{ \frac{1}{432}(1 - y^4)(581 + 6140y^2 + 581y^4) \right. \\ &\quad - \frac{\pi^2}{36}(7 - 6y + 28y^2 + 222y^3 - 164y^4 + 390y^5 - 140y^6 + 66y^7 - 5y^8) \\ &\quad - \frac{1}{36}(1 - y^4)(13 - 176y^2 + 13y^4) \ln(1 - y^2) + \frac{1}{3}y^2(2 + 46y^2 + 38y^4 + y^6) \ln^2 y \\ &\quad + \frac{2}{3}y(1 - y)^4(5 - 4y + 5y^2) \ln(1 - y) \ln y - \frac{2}{3}y(1 + y)^4(5 + 4y + 5y^2) \ln(1 + y) \ln y \\ &\quad + \frac{1}{18}y^2(212 + 930y^2 + 388y^4 - 13y^6) \ln y \\ &\quad + \frac{1}{3}(1 - 10y - 56y^2 - 102y^3 - 164y^4 - 102y^5 - 56y^6 - 10y^7 + y^8)\text{Li}_2(-y) \\ &\quad \left. + \frac{1}{3}(1 + 10y - 56y^2 + 102y^3 - 164y^4 + 102y^5 - 56y^6 + 10y^7 + y^8)\text{Li}_2(y) \right\}. \quad (38) \end{aligned}$$

i	$\mu \rightarrow e$			$\tau \rightarrow \mu$			$\tau \rightarrow e$		
	$\delta\hat{G}_i^{<}$	$\delta\hat{G}_i^{>}$	$\delta\hat{G}_i$	$\delta\hat{G}_i^{<}$	$\delta\hat{G}_i^{>}$	$\delta\hat{G}_i$	$\delta\hat{G}_i^{<}$	$\delta\hat{G}_i^{>}$	$\delta\hat{G}_i$
1	+2.80%	-2.69%	-0.42%	+0.76%	-1.14%	-0.40%	+ 5.20%	-4.44%	-0.42%
2	+8.22%	-3.70%	-0.68%	+2.51%	-1.59%	-0.62%	+14.70%	-6.10%	-0.68%
3	+2.56%	-2.68%	-0.53%	+0.66%	-1.14%	-0.45%	+ 4.95%	-4.43%	-0.54%
4	+7.82%	-3.70%	-0.79%	+2.53%	-1.59%	-0.67%	+14.28%	-6.10%	-0.80%

Table 2:

Numerical values of partially integrated ($\delta\hat{G}_i^{<}$, $\delta\hat{G}_i^{>}$) and total rate functions ($\delta\hat{G}_i$) divided by their respective Born term values. The symbols “<” and “>” stand for integrations from threshold to the zero point of the respective $O(\alpha)$ contributions, and from the zero point to the endpoint of the spectrum.

Note that $\hat{G}_2^{(\alpha)}$ and $\hat{G}_3^{(\alpha)}$ contain trilog functions, whereas $\hat{G}_1^{(\alpha)}$ and $\hat{G}_4^{(\alpha)}$ contain only dilog functions. In agreement with the Lee-Nauenberg theorem [3] the rate functions do not contain any logarithmic mass singularities. Our results for \hat{G}_1 agree with the result in [20] where a different route of phase space integrations was taken to arrive at the total rate. Our results for \hat{G}_2 agree with those in [7]. The results on \hat{G}_3 and \hat{G}_4 are new. In addition, we have checked that all four rate functions $\hat{G}_i^{(\alpha)}$ vanish for $y = 1$.

In order to get a quantitative feeling about the size of the radiative corrections to the respective spectrum functions we have listed in Table 2 the percentage changes $\delta\hat{G}_i$ induced by the radiative corrections, where

$$\delta\hat{G}_i = \frac{(\hat{G}_i^{(\alpha)} + \hat{G}_i^{Born}) - \hat{G}_i^{Born}}{\hat{G}_i^{Born}} = \frac{\hat{G}_i^{(\alpha)}}{\hat{G}_i^{Born}}. \quad (39)$$

The relative radiative corrections $\delta\hat{G}_i$ can all be seen to be close to the naive expectation of order α . However, as was emphasized earlier on, all radiative corrections discussed in this paper go through zeros. Integrating over the whole spectrum may therefore not give an adequate representation of the size of the radiative corrections since there are sizable cancellation effects. This cancellation would become less effective if moments of the spectrum functions were taken. The moments could be chosen such that they either emphasize the threshold or the endpoint region. Alternatively, one can consider partially integrated rates where the integrations either run from threshold to the point where the radiative corrections go to zero or from the zero point to the endpoint. The two partially

integrated rate functions will be denoted by $\hat{G}_i^<$ (lower part) and by $\hat{G}_i^>$ (upper part). The two respective partially integrated relative rate functions $\delta\hat{G}_i^<$ and $\delta\hat{G}_i^>$ are also listed in Table 2. The relative radiative corrections for the partially integrated rate functions can be seen to be much larger than for the fully integrated rate functions and can amount up to $O(10\%)$. Note, though, that, in contrast to the rate functions, neither the moments of the spectral functions nor the partially integrated rates are free of logarithmic mass singularities.

Since the complete rate expressions are rather unwieldy it is useful to consider the small y -expansions of the rate expressions. One has

$$\hat{G}_1^{(\alpha)} = \frac{\alpha}{\pi} \left\{ \frac{25 - 4\pi^2}{16} - (17 + 12 \ln y)y^2 + 8\pi^2 y^3 + O(y^4) \right\}, \quad (40)$$

$$\begin{aligned} \hat{G}_2^{(\alpha)} = \frac{\alpha}{\pi} \left\{ -\frac{617 - 84\pi^2}{432} - \frac{2}{3}y - \frac{1}{3}(24 - 2\pi^2 - \ln y)y^2 + \right. \\ \left. + \frac{2}{27}(71 + 84 \ln y)y^3 + O(y^4) \right\}, \end{aligned} \quad (41)$$

$$\begin{aligned} \hat{G}_3^{(\alpha)} = \frac{\alpha}{\pi} \left\{ -\frac{21 - 4\pi^2}{16} - \frac{10}{3}y - \frac{1}{27}(232 + 6\pi^2 + 87 \ln y + \right. \\ \left. + 36 \ln^2 y)y^2 + \frac{2}{9}(121 - 84 \ln y)y^3 + O(y^4) \right\}, \end{aligned} \quad (42)$$

$$\begin{aligned} \hat{G}_4^{(\alpha)} = \frac{\alpha}{\pi} \left\{ \frac{7(83 - 12\pi^2)}{432} + \frac{1}{6}y + \frac{1}{27}(578 - 21\pi^2 + 138 \ln y + \right. \\ \left. + 18 \ln^2 y)y^2 - \frac{37}{6}\pi^2 y^3 + O(y^4) \right\}. \end{aligned} \quad (43)$$

It is well-known that the $O(\alpha)$ small- y corrections to the reduced rate $\hat{G}_1^{(\alpha)}$ start only at $O(y^2)$ (see e.g. [17, 21]). In contradistinction the mass corrections to the spin dependent rate functions $\hat{G}_2^{(\alpha)}$, $\hat{G}_3^{(\alpha)}$ and $\hat{G}_4^{(\alpha)}$ all start at $O(y)$ due to the lower integration limit $x = 2y$. In order to obtain a quantitative feeling about the importance of mass effects in the $O(\alpha)$ radiative contributions we have listed in Table 1 the percentage changes in the rate functions \hat{G}_i when going from $m_\nu \rightarrow 0$ to $m_\nu \neq 0$ using the $m_\nu \rightarrow 0$ results listed in Sec. 6. The mass effects are not small, in particular for the case ($\tau \rightarrow \mu$). The percentage changes for the radiative contributions are larger than those in the Born term case which

is partly due to the difference in the power pattern of the final state mass corrections in the two cases. The quality of the $m_{l'} \rightarrow 0$ approximation for the radiative corrections can be assessed by referring again to Table 1. Final state mass effects tend to reduce the overall size of the radiative corrections. The reduction is largest ($O(10\%)$) for the case ($\tau \rightarrow \mu$) and smallest ($O(10^{-1})$) for the case ($\tau \rightarrow e$). They are largest for the rate functions \hat{G}_3 and \hat{G}_4 and smallest for \hat{G}_1 . That the mass effects are smallest for \hat{G}_1 is due to the fact that the mass corrections to \hat{G}_1 set in only at $O(y^2)$ (see Eq. (34)). Whether one is willing to tolerate the error incurred in using the simpler $m_{l'} \rightarrow 0$ radiative correction formulas depends of course on the accuracy required for the application at hand.

We now turn to the discussion of the average longitudinal polarization of the electron $\langle P_e^l \rangle$ and the average forward-backward asymmetry $\langle A_{FB} \rangle$. They take remarkably simple forms in the $y \rightarrow 0$ limit. Including the Born term contribution and expanding the inverse denominator in powers of α/π one has

$$\langle P_e^l \rangle = -\left(1 - \frac{\alpha}{2\pi}\right). \quad (44)$$

Note that $\langle P_e^l \rangle$ does not depend on $P \cos \theta_P$ in this approximation.

In the case of the average forward-backward asymmetry one has to distinguish between the two cases $\cos \theta \neq 1$ and $\cos \theta = 1$. For $\cos \theta \neq 1$ one obtains

$$\langle A_{FB} \rangle = -\frac{1}{3} \left(1 - \frac{\alpha}{\pi} \frac{6\pi^2 - 49}{9}\right) P. \quad (45)$$

The case $\cos \theta = 1$ is special since the $O(y^0)$ Born term contributions in the numerator and denominator of A_{FB} cancel. One finds

$$\langle A_{FB} \rangle = -\frac{16y^2 + \frac{\alpha}{\pi}}{32y^2 + \frac{\alpha}{\pi}3} P, \quad (46)$$

where we have included the $O(y^2)$ Born term contribution. For ($\mu \rightarrow e$) and ($\tau \rightarrow e$) the $O(\alpha)$ contribution dominates and one obtains $A_{FB} = -1/3$. For ($\tau \rightarrow \mu$) the $O(y^2)$ contribution in (46) dominates and one obtains $A_{FB} = -1/2$. Note that $\langle A_{FB} \rangle$ does not depend on $\cos \theta$ except for values close to $\cos \theta = 1$. The actual numerical values for $\langle P_e^l \rangle$ and for $\langle A_{FB} \rangle$ lie very close to the above first order estimates in all cases.

6 The $m_e \rightarrow 0$ limit and the anomalous helicity flip contribution

The purpose of this section is two-fold. First we discuss the $m_e \rightarrow 0$ limit of the $m_e \neq 0$ $O(\alpha)$ results given in Sec. 5. This allows us to make contact with the $m_e \rightarrow 0$ results derived previously [6]. Second we discuss in some detail the origin of the anomalous helicity flip contribution resulting from collinear photon emission of the electron. Our results are presented in terms of the two diagonal components of the density matrix of the final state electron, which, in the limit $m_e \rightarrow 0$, are nothing but the helicity no-flip and helicity flip contributions of the final state electron. The naive prediction of massless Quantum-*Electro*-Dynamics is that the helicity flip contributions vanish in all orders of perturbation theory. However, as first pointed out by Lee and Nauenberg [3], there will be a nonzero helicity flip contribution from collinear photon emission which survives the $m_e \rightarrow 0$ limit. This will be demonstrated in our $O(\alpha)$ $m_e \rightarrow 0$ expressions. Our $m_e \rightarrow 0$ result for the helicity flip contribution is found to be in agreement with expectations derived from the universal equivalent particle approach of Falk and Sehgal [5]. For a discussion of the quality of the $m_l \rightarrow 0$ approximation for the three cases ($\mu \rightarrow e$), ($\tau \rightarrow \mu$) and ($\tau \rightarrow e$) we refer to the discussion at the end of Sec. 5.

Since we want to discuss the helicity no-flip and flip contributions separately it is convenient to choose a slightly different representation for the differential rate Eq. (1). We write the differential rate in terms of the no-flip and flip contributions

$$\frac{d\Gamma}{dx d\cos\theta_P} = \frac{d\Gamma^{nf}}{dx d\cos\theta_P}(1 - \cos\theta) + \frac{d\Gamma^{hf}}{dx d\cos\theta_P}(1 + \cos\theta), \quad (47)$$

where the no-flip and flip contributions are given by

$$\frac{d\Gamma^{nf/hf}}{dx d\cos\theta_P} = \frac{1}{2}\beta x \Gamma_0 \left((G_1 \mp G_3) + (G_2 \mp G_4)P \cos\theta_P \right). \quad (48)$$

The terminology helicity no-flip (*nf*) and helicity flip (*hf*) is really only appropriate in the $m_e \rightarrow 0$ limit where the electron emerging from the left-chiral weak interaction current is purely left-handed. After photon emission the electron can then remain left-handed (*nf*) or can become right-handed (*hf*). For $m_e \neq 0$ the respective *nf/hf* contributions are nothing but the (unnormalized) diagonal elements of the density matrix of the electron, i.e. $\Gamma^{nf} \sim \rho_{--}$ and $\Gamma^{hf} \sim \rho_{++}$.

As concerns the helicity flip contribution one notes that there are no Born term helicity flip contributions in the limit $m_e = 0$ since a massless electron emerging from the weak ($V - A$) vertex is left-handed. This is explicitly seen by inserting the Born term rate

functions Eq. (13) in Eq. (48). Naively, one would expect no helicity flip contributions also at $O(\alpha)$ because, in massless QED with $m_e = 0$, photon emission from the electron is helicity conserving. However, taking the limit $m_e \rightarrow 0$ in Eqs. (27) - (30) one finds helicity flip contributions which survive the $m_e \rightarrow 0$ limit. In fact, one finds

$$\frac{d\Gamma^{hf}}{dx d\cos\theta_P} = \frac{\alpha}{12\pi}\Gamma_0\left(\left[(1-x)^2(5-2x)\right] - \left[(1-x)^2(1+2x)\right]P\cos\theta_P\right), \quad (49)$$

which agrees with the result presented in Ref. [6]. Because of the naive expectation that the helicity flip contribution vanishes in massless QED the presence of a helicity flip contribution is sometimes referred to as the anomalous helicity flip contribution. Moreover, the authors of Ref. [22] were able to show that the well-known axial anomaly can be traced back to the existence of an anomalous helicity flip contribution to the absorptive part of the VVA triangle diagram in massless QED. This gives further justification for the use of the phrase ‘‘anomalous helicity flip contribution’’. In order to set the anomalous contributions apart we have highlighted them in Eq. (49) by enclosing them in square brackets.

The authors of Ref. [6] had already expressed surprise at the simplicity of the structure of the $O(\alpha)$ helicity flip contributions without, however, attempting to identify the source of this structural simplicity. The simplicity of the helicity flip contribution becomes manifest in the equivalent particle description of μ -decay where, in the peaking approximation, μ -decay is described by the two-stage process $\mu^- \rightarrow e^-$ followed by the branching process $e^- \rightarrow e^- + \gamma$ characterized by universal splitting functions $D_{nf/hf}(z)$ [5]. In the splitting process z is the fractional energy of the emitted photon [5]. The off-shell electron in the propagator is replaced by an equivalent on-shell electron in the intermediate state. Since the helicity flip contribution arises entirely from the collinear configuration it can be calculated in its entirety using the equivalent particle description.

The helicity flip splitting function is given by $D_{hf}(z) = \alpha z/(2\pi)$, where $z = k_0/E' = (E' - E)/E' = 1 - x/x'$, and where k_0 is the energy of the emitted photon [5]. E' and E denote the energies of the initial and final electron in the splitting process. The helicity flip splitting function has to be folded with the appropriate $m_e = 0$ Born term contribution. The lower limit of the folding integration is determined by the soft photon point where $E' = E$. The upper limit is determined by the maximal energy of the initial electron $E' = m_\mu/2$. One obtains

$$\frac{d\Gamma^{hf}}{dx d\cos\theta_P} = \frac{\alpha}{2\pi} \int_x^1 dx' \frac{1}{x'} \frac{d\Gamma^{Born;nf}(x')}{dx' d\cos\theta_P} \left(1 - \frac{x}{x'}\right)$$

$$\begin{aligned}
&= \frac{\alpha}{2\pi} \Gamma_0 \int_x^1 dx' (x' - x) \left((3 - 2x') + (1 - 2x') P \cos \theta_P \right) \\
&= \frac{\alpha}{12\pi} \Gamma_0 \left((1 - x)^2 (5 - 2x) - (1 - x)^2 (1 + 2x) P \cos \theta_P \right), \tag{50}
\end{aligned}$$

which exactly reproduces the result of Eq. (49). Integrating over the spectrum one obtains

$$\frac{d\Gamma^{hf}}{d\cos \theta_P} = \frac{\alpha}{\pi} \Gamma_0 \left(\left[\frac{1}{8} \right] - \left[\frac{1}{24} \right] P \cos \theta_P \right). \tag{51}$$

Taking the forward-backward asymmetry of the helicity flip contribution (51) one reproduces the $\cos \theta = 1$ result of Eq. (46) (for $y^2 = 0$).

The helicity no-flip contribution is again obtained by taking the $m_e \rightarrow 0$ limit in Eqs. (27) - (30) but now for the differences of the respective spectrum functions as specified in Eq. (48). Including the $O(y^0)$ Born term contributions one obtains

$$\begin{aligned}
\frac{d\Gamma^{nf}}{dx d\cos \theta_P} &= \Gamma_0 \left(x^2 (3 - 2x) + \frac{\alpha}{12\pi} \left\{ - \left[(1 - x)^2 (5 - 2x) \right] - 4x(11 - 10x + 5x^2) \right. \right. \\
&\quad - 6(6 - x)x \ln(1 - x) - 2(5 + 12x - 15x^2 + 4x^3) \ln \left(\frac{y}{x} \right) \\
&\quad \left. \left. + 6(3 - 4x)x^2 \ln \left(\frac{y}{1 - x} \right) + 12(3 - 2x)x^2 \sigma \right\} \right. \\
&\quad + \left(x^2 (1 - 2x) + \frac{\alpha}{12\pi} \left\{ \left[(1 - x)^2 (1 + 2x) \right] - 2(3 - 10x - 13x^2 + 8x^3) \right. \right. \\
&\quad - \frac{2}{x} (4 - 12x + 18x^2 - 13x^3) \ln(1 - x) + 2(1 + 21x^2 - 4x^3) \ln \left(\frac{y}{x} \right) \\
&\quad \left. \left. + 6(1 - 4x)x^2 \ln \left(\frac{y}{1 - x} \right) + 12(1 - 2x)x^2 \sigma \right\} \right) P \cos \theta_P \Big), \tag{52}
\end{aligned}$$

where

$$\sigma = -\frac{\pi^2}{3} + 2\text{Li}_2(x) + \ln(x) \ln(1 - x) + 2 \ln \left(\frac{x}{1 - x} \right) \ln \left(\frac{y}{x} \right). \tag{53}$$

The no-flip contribution agrees with the result presented in Ref. [6]. We have highlighted the anomalous contributions in Eq.(52) by enclosing them in square brackets. When calculating the total rate, i.e. when summing the flip and no-flip contributions (49) and (52), the anomalous contributions cancel.

The longitudinal polarization of the daughter electron takes a rather simple form in the $m_e \rightarrow 0$ limit when one expands out the inverse denominator in terms of powers of (α/π) keeping only the $O(\alpha)$ contribution. In terms of the flip and no-flip contributions the longitudinal polarization of the electron reads

$$P_e^l = \frac{d\Gamma^{hf} - d\Gamma^{nf}}{d\Gamma^{hf} + d\Gamma^{nf}} \quad (54)$$

When expanding the inverse denominator in terms of powers of (α/π) one sees that the “normal” contributions in the numerator and denominator cancel exactly at $O(\alpha)$ and one just remains with the anomalous contributions (No such cancellations occur for the forward-backward asymmetry A_{FB} . We therefore refrain from presenting a closed formula for A_{FB} in this approximation). One obtains

$$P_e^l = -\left(1 - \frac{\alpha}{6\pi} \frac{(1-x)^2}{x^2} \frac{5-2x - (1+2x)P \cos \theta_P}{3-2x + (1-2x)P \cos \theta_P}\right) \quad (55)$$

It is clear that Eq.(55) does not apply very close to threshold. Due to the factor $(1-x)^2/x^2$ in (55) the radiative corrections to the longitudinal polarization of the daughter lepton are largest close to threshold as is evidenced in the plots Fig. 1b and Fig. 3b. In the case of $(\tau \rightarrow \mu)$ mass effects prevent the radiative corrections to become large in the threshold region.

Integrating the no-flip contribution over the spectrum one obtains

$$\frac{d\Gamma^{nf}}{d\cos \theta_P} = \Gamma_0 \left(\frac{1}{2} + \frac{\alpha}{\pi} \left(-\left[\frac{1}{8} \right] + \frac{25}{16} - \frac{1}{4}\pi^2 \right) + \left(-\frac{1}{6} + \frac{\alpha}{\pi} \left(\left[\frac{1}{24} \right] - \frac{617 - 84\pi^2}{432} \right) \right) P \cos \theta_P \right). \quad (56)$$

Taking the forward-backward asymmetry of (56) one reproduces the $\cos \theta = 1$ result Eq. (45). We have again highlighted the anomalous contributions by enclosing them in square brackets. The anomalous contributions can be seen to cancel in the spectrum and rate functions when adding up the spectrum no-flip contribution (52) and flip contribution (49), and the respective rate contributions (56) and (51). Numerically the $O(\alpha)$ no-flip contribution dominates over the $O(\alpha)$ (anomalous) flip contribution. For the $O(\alpha)$ contributions to the rate functions, which do not depend on y , one obtains $(-0.168, -0.121, -0.107)$ for the rate ratio $d\Gamma^{hf}/d\Gamma^{nf}$, for $\cos \theta_P = 1, 0, -1$.

7 Summary and conclusions

We have computed the $O(\alpha)$ corrections to the leptonic decays of the μ - and τ -leptons including polarization effects and the full mass dependence of the respective final-state leptons. The radiative corrections to the spectrum functions are sizeable for $(\mu \rightarrow e)$ -decays, large for $(\tau \rightarrow e)$ -decays, and smaller for $(\tau \rightarrow \mu)$ -decays. In large part this pattern is due to the $\ln y$ dependent contributions in the spectrum. The longitudinal polarization of the final-state lepton deviates substantially from the naive value of $P_{\nu}^l = -1$ towards the soft end of the spectrum. The radiative corrections to the longitudinal polarization of the daughter lepton in the threshold region are substantial for $(\mu \rightarrow e)$ - and $(\tau \rightarrow e)$ -decays and small for $(\tau \rightarrow \mu)$ -decays. Similar statements hold for the forward-backward asymmetry A_{FB} where the case $\cos\theta = 1$ plays a special role.

For the rate functions we have compared our $O(\alpha)$ $m_{\nu} \neq 0$ results with $m_{\nu} \rightarrow 0$ results derived previously in [6]. In particular in the $(\tau \rightarrow \mu)$ case the errors incurred in using the $O(\alpha)$ $m_{\nu} \rightarrow 0$ results are large (of $O(10\%)$ in the rate functions). Whether one is willing to tolerate the error brought about by using the simpler $m_{\nu} \rightarrow 0$ radiative correction formulas depends of course on the accuracy required for the application at hand. We nevertheless strongly recommend use of the complete results in numerical investigations instead of using the $m_{\nu} \rightarrow 0$ approximation. The analytical $m_{\nu} \neq 0$ formulas written down in this paper are of sufficient simplicity to allow for easy incorporation into numerical programs.

Acknowledgements: We acknowledge informative discussions with F. Scheck, K. Schilcher and H. Spiesberger. We would like to thank A.B. Arbuzov for clarifying e-mail exchanges. M.C. Mauser was supported by the DFG (Germany) through the Graduiertenkolleg ‘‘Eichtheorien’’ at the University of Mainz. S. Groote acknowledges support through the DFG.

A Appendix A

When integrating the spectrum functions it is convenient to transform to the integration variable ξ , where $x = y(\xi^2 + 1)/\xi$ such that $\beta = (1 - \xi^2)/(1 + \xi^2)$.

Trilog functions are generated from the integrals

$$\int_1^y \frac{1}{\xi} \ln(\xi) \ln(\xi - y) d\xi = \frac{\pi^2}{6} \ln y + \frac{1}{3} \ln^3 y - \text{Li}_3(y) + \zeta(3), \quad (\text{A1})$$

$$\int_1^y \frac{1}{\xi} \ln(\xi) \ln(1 - y\xi) d\xi = -\ln(y) \text{Li}_2(y^2) - \text{Li}_3(y) + \text{Li}_3(y^2), \quad (\text{A2})$$

$$\int_1^y \frac{1}{\xi} \text{Li}_2\left(\frac{y(1-\xi^2)}{\xi(1-y\xi)}\right) d\xi = \frac{1}{2} \ln(y) \text{Li}_2(y^2) + 2 \text{Li}_3(y) - \text{Li}_3(y^2) - \zeta(3), \quad (\text{A3})$$

$$\int_1^y \frac{1}{\xi} \text{Li}_2\left(\frac{1-\xi^2}{1-y\xi}\right) d\xi = \frac{\pi^2}{6} \ln y - \frac{1}{2} \ln(y) \text{Li}_2(y^2) - 2 \text{Li}_3(y) + \text{Li}_3(y^2) + \zeta(3), \quad (\text{A4})$$

where

$$\text{Li}_2(x) := -\int_0^1 \frac{\ln(1-y)}{y} dy, \quad \text{Li}_3(x) := \int_0^1 \frac{\text{Li}_2(y)}{y} dy. \quad (\text{A5})$$

Use has been made of the relation

$$\text{Li}_n(x) + \text{Li}_n(-x) = \frac{1}{2^{n-1}} \text{Li}_n(x^2). \quad (\text{A6})$$

Euler's *Zeta* function is defined by

$$\zeta(s) = \sum_{k=1}^{\infty} k^{-s}, \quad \zeta(3) = 1.202057\dots \quad (\text{A7})$$

B Appendix B

The Fierz identity

$$[\gamma^\mu(1-\gamma_5)]_{\alpha\beta} [\gamma_\mu(1-\gamma_5)]_{\gamma\delta} = -[\gamma^\mu(1-\gamma_5)]_{\gamma\beta} [\gamma_\mu(1-\gamma_5)]_{\alpha\delta} \quad (\text{B1})$$

is well known. Not so well known is the Fierz identity

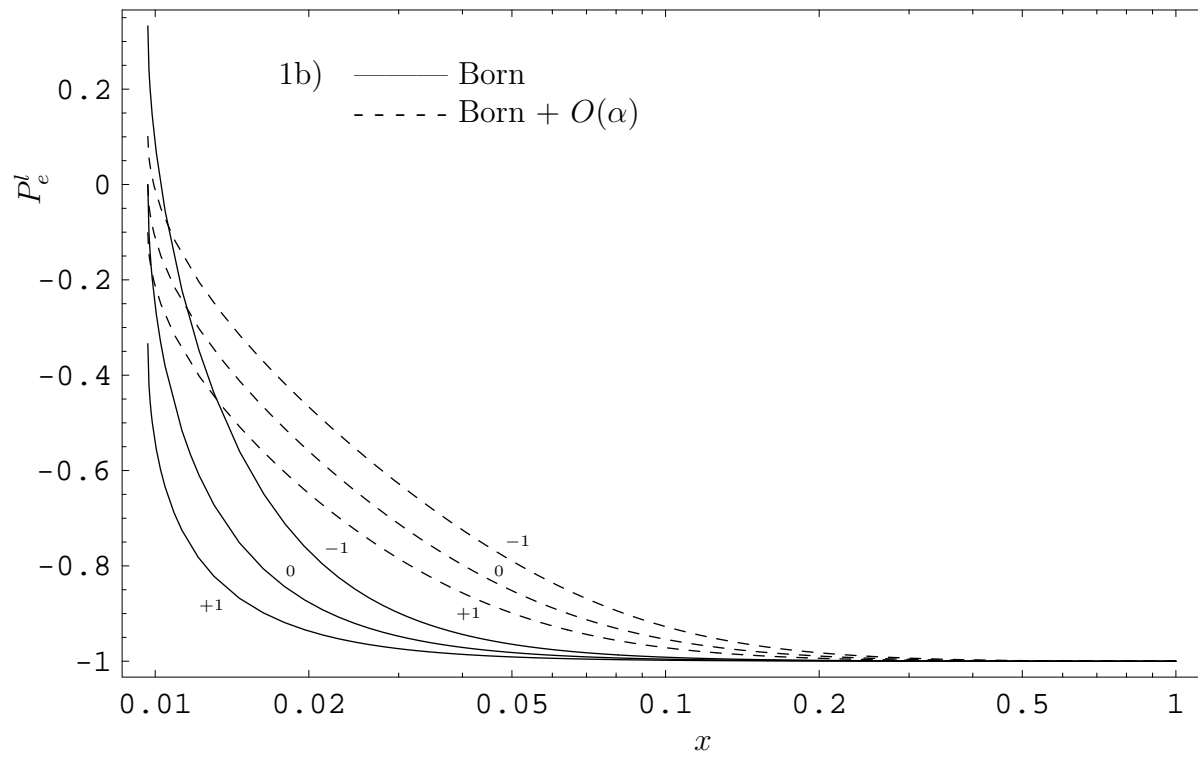
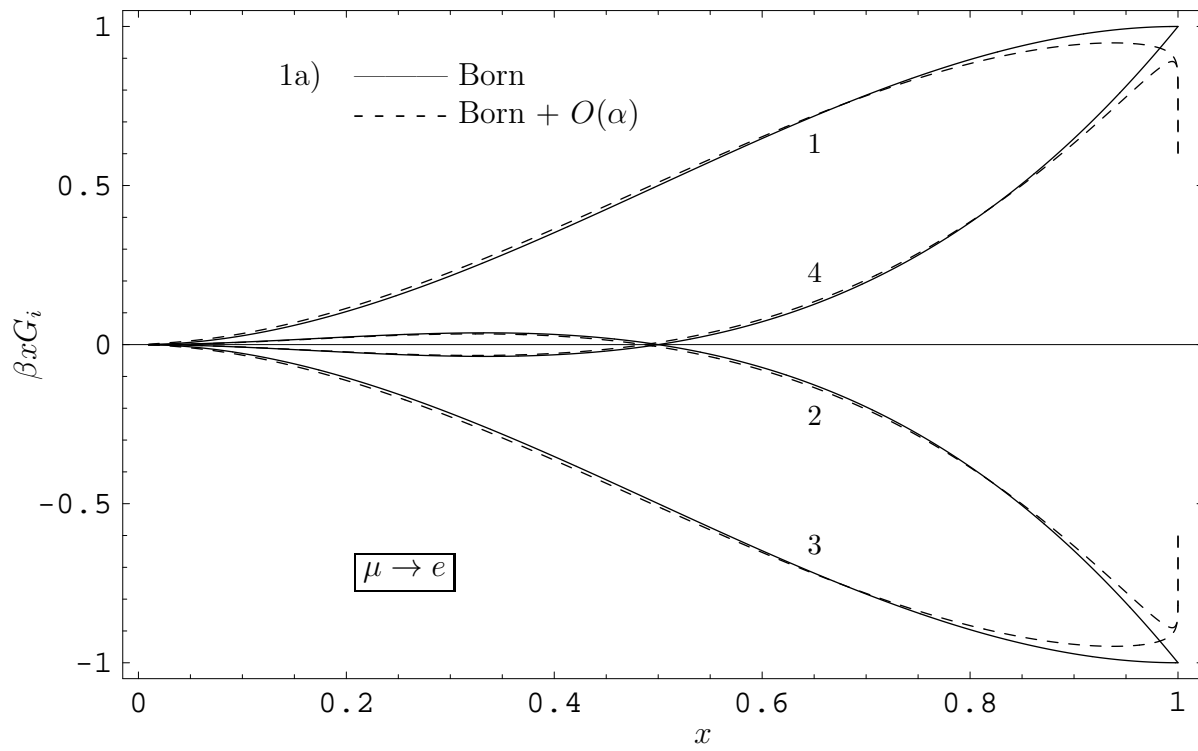
$$[(1\pm\gamma_5)]_{\alpha\beta} [(1\mp\gamma_5)]_{\gamma\delta} = \frac{1}{2} [\gamma^\mu(1\mp\gamma_5)]_{\gamma\beta} [\gamma_\mu(1\pm\gamma_5)]_{\alpha\delta}. \quad (\text{B2})$$

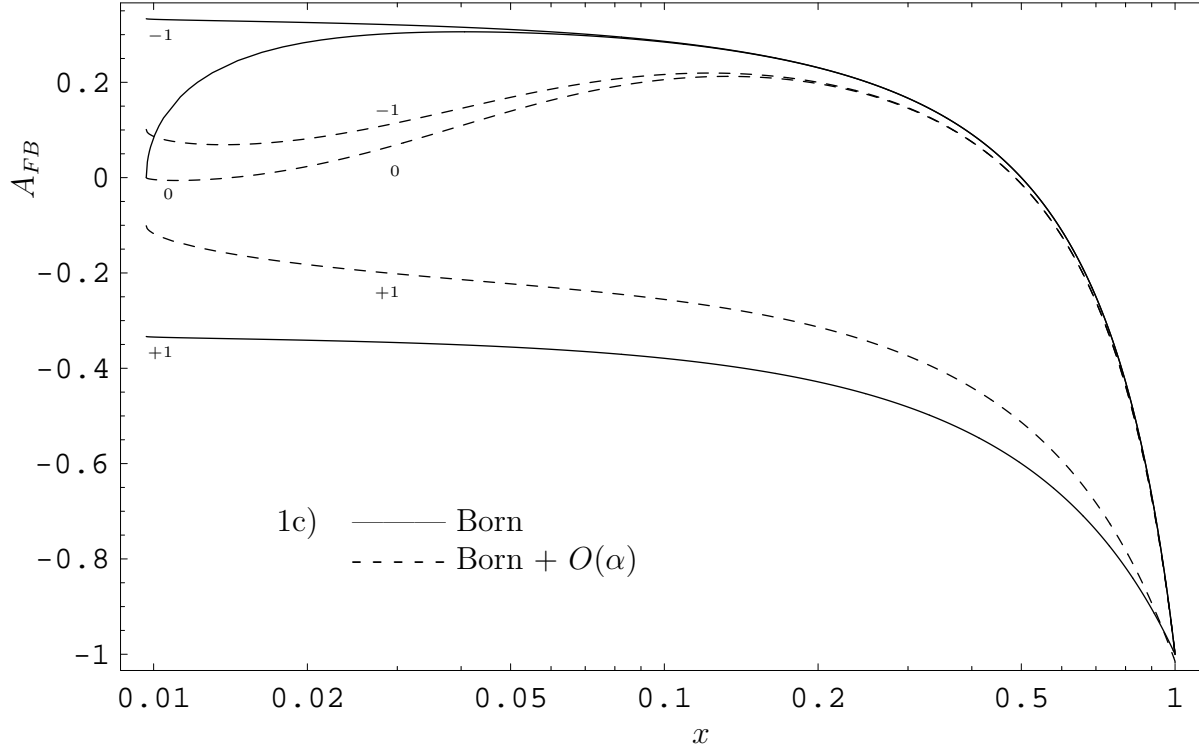
Latter identity allows one to transform the $q^\mu q^\nu$ piece of the W -boson propagator discussed in Sec. 4 back into the standard form $N^{\alpha\beta} C_{\alpha\beta}$ used in the remaining part of the paper.

References

- [1] M. Fischer, S. Groote, J.G. Körner and M.C. Mauser, Phys. Lett. **B480** (2000) 265.
- [2] M. Fischer, S. Groote, J.G. Körner and M.C. Mauser, **hep-ph/0101322**,
to be published in Phys. Rev. **D65** (2002) 013205.
- [3] T.D. Lee and M. Nauenberg, Phys. Rev. **133B** (1964) 1549;
- [4] A.V. Smilga, Commun. Nucl. Part. Phys. **20** (1991) 69;
J.G. Körner, A. Pilaftsis and M.M. Tung, Z. Phys. **C63** (1994) 575;
S. Groote, J.G. Körner and M.M. Tung, Z. Phys. **C74** (1997) 615;
S. Groote, J.G. Körner and J.A. Leyva, Phys. Lett. **B418** (1998) 192;
L. Trentadue and M. Verbeni, Phys. Lett. **B478** (2000) 137 and
Nucl. Phys. **B583** (2000) 307.
- [5] B. Falk and L.M. Sehgal, Phys. Lett. **B325** (1994) 509.
- [6] W.E. Fischer and F. Scheck, Nucl. Phys. **B83** (1974) 25.
- [7] A.B. Arbuzov, Phys. Lett. **B524** (2002) 99
- [8] G. Källén, “Elementary Particle Physics”, Addison-Wesley Publishing Company,
Reading, Massachusetts, USA, 1964.
- [9] E.D. Commins and P.H. Bucksbaum, “Weak Interactions of Leptons and Quarks”,
Cambridge University Press, Cambridge, U.K., 1983.
- [10] F. Scheck, “Leptons, Hadrons and Nuclei”, North Holland Physics Publishing,
Amsterdam, 1983.
- [11] T.D. Lee and C.S. Wu, Annual Review of Nuclear Science **15** (1965) 381;
ibid **16** (1966) 471.
- [12] G. Källén, Springer Tracts in Modern Physics **46** (1968) 67.
- [13] F. Scheck, Phys. Rep. **44** (1978) 187.

- [14] D. E. Groom *et al.* [Particle Data Group Collaboration],
Eur. Phys. J. **C19** (2000) 1.
- [15] W. J. Marciano and A. Sirlin, Phys. Rev. Lett. **61** (1988) 1815.
- [16] K. Schilcher, M.D. Tran and N.F. Nasrallah, Nucl.Phys. **B181** (1981) 91,
Erratum *ibid.* **B187** (1981) 594;
G.J. Gounaris and J.E. Paschalis, Nucl. Phys. **B222** (1983) 473.
- [17] M. Roos and A. Sirlin, Nucl. Phys. **B29** (1971) 296.
- [18] E. Kuraev and V.S. Fadin, Sov. J. Nucl. Phys. **41** (1985) 466,
[Yad. Fiz. 41 (1985) 733].
- [19] M. Cacciari, A. Deandrea, G. Montagna and O. Nicrosini,
Europhys. Lett. **17** (1992) 123.
- [20] Y. Nir, Phys. Lett. **B221** (1989) 184.
- [21] T. van Ritbergen and R.G. Stuart, Nucl. Phys. **B564** (2000) 343.
- [22] A.D. Dolgov and V.I. Zakharov, Nucl. Phys. **B27** (1971) 525.





Figures 1a,b,c:

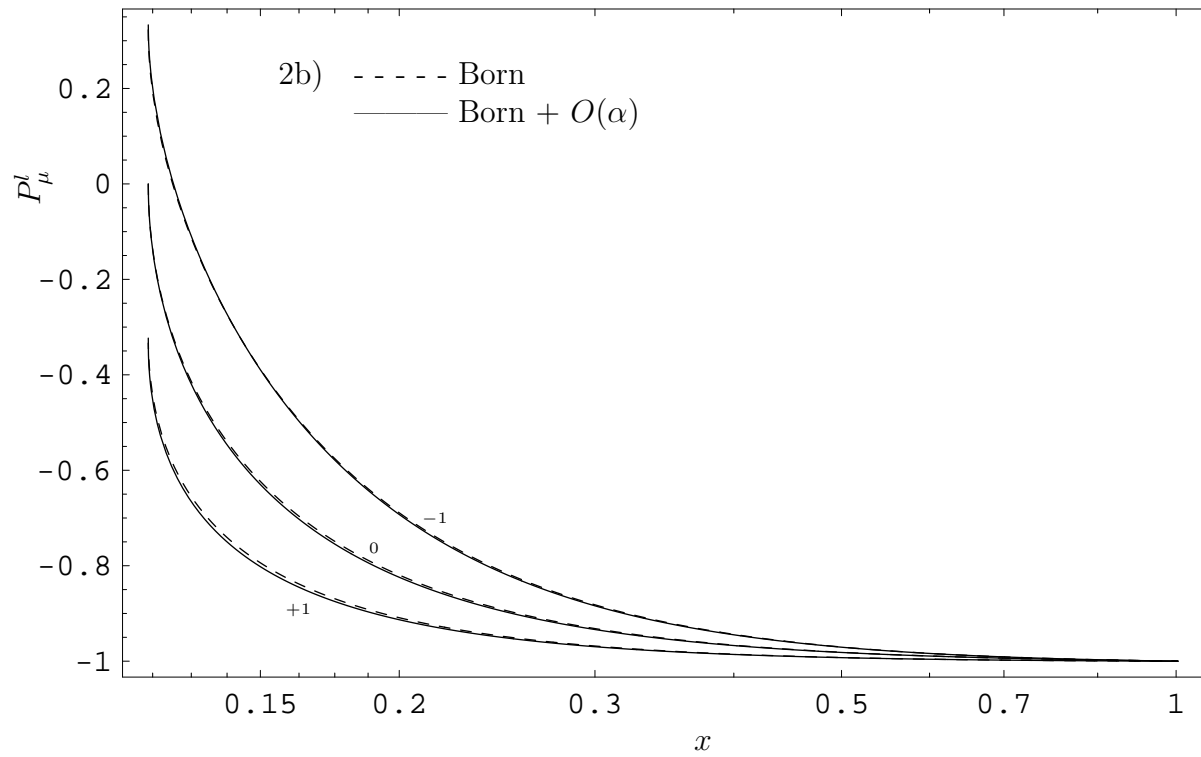
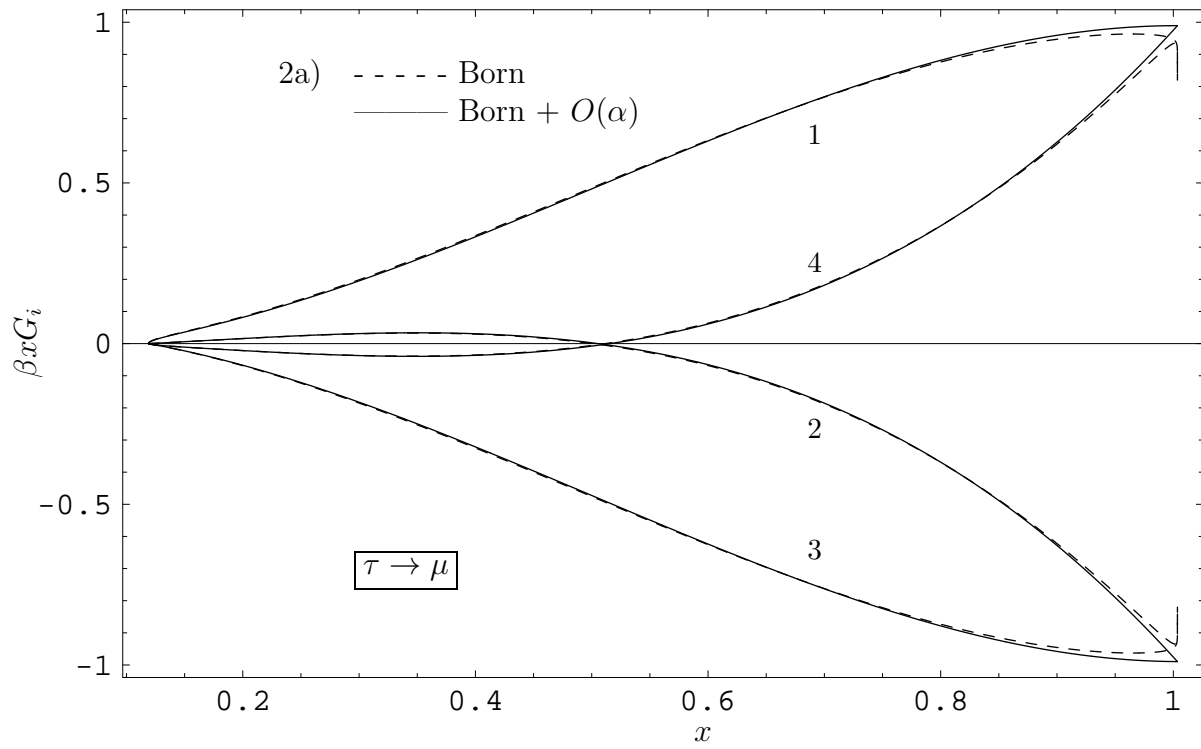
The case $\mu \rightarrow e$. Scaled energy dependence of

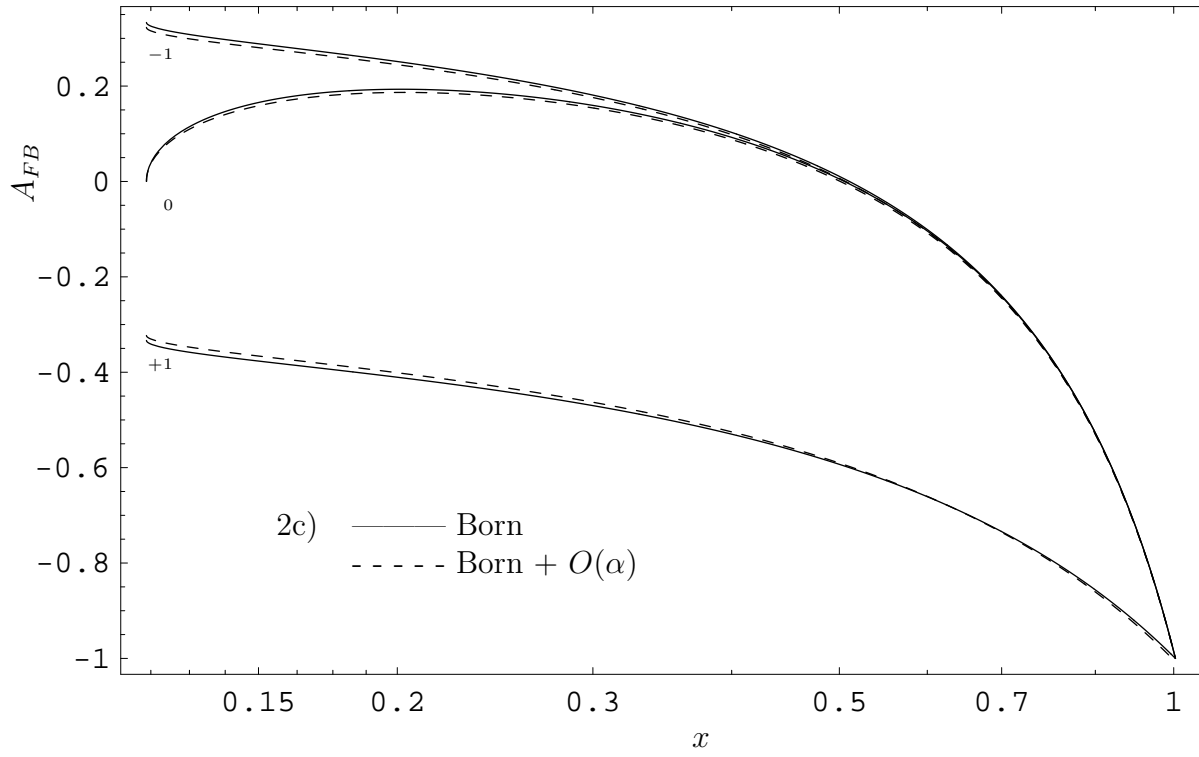
(a) spectrum functions $\beta x G_i$,

(b) the longitudinal polarization of the electron P_e^l for $\cos \theta_P = -1, 0, +1$, and

(c) the forward-backward asymmetry A_{FB} for $\cos \theta = -1, 0, +1$.

All curves with and without radiative corrections. Polarisation P is set to $P = 1$.

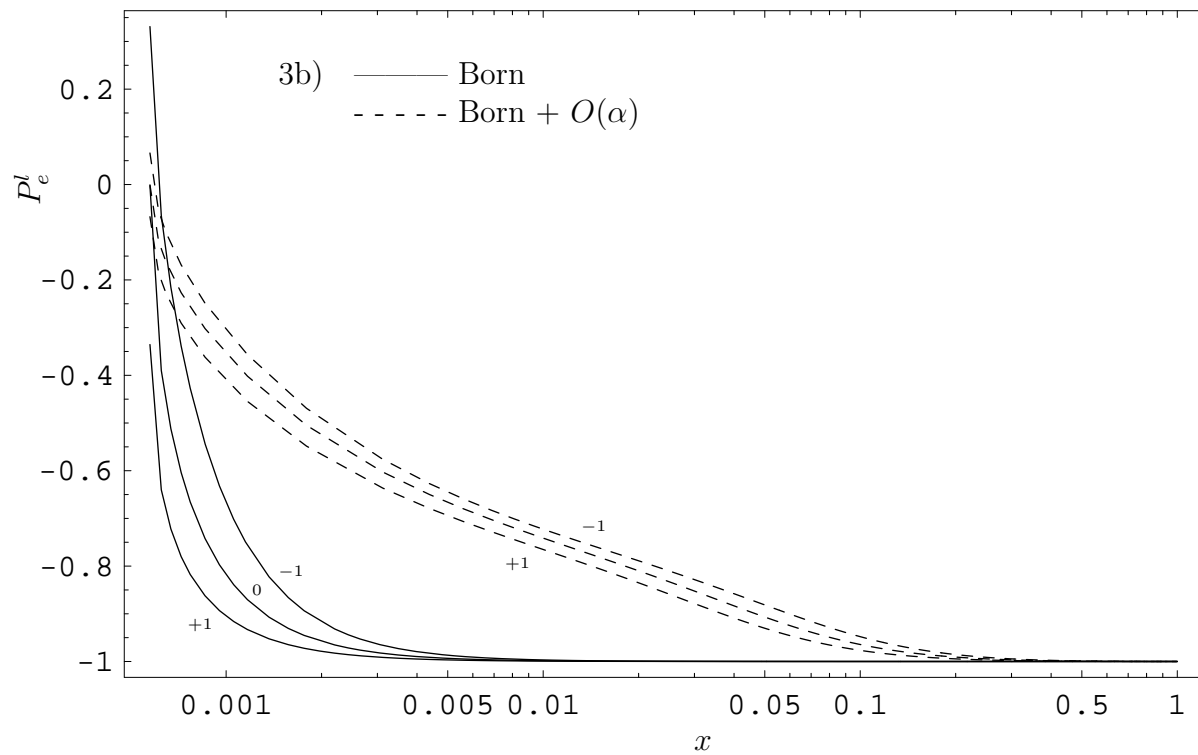
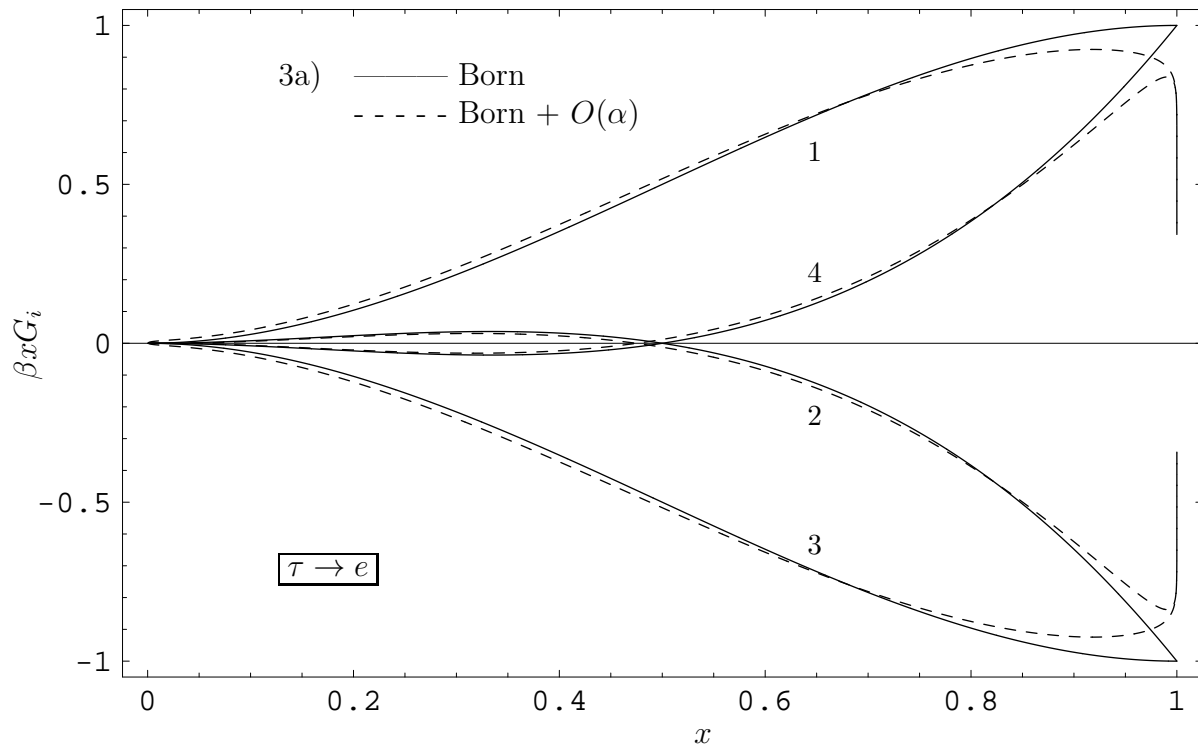


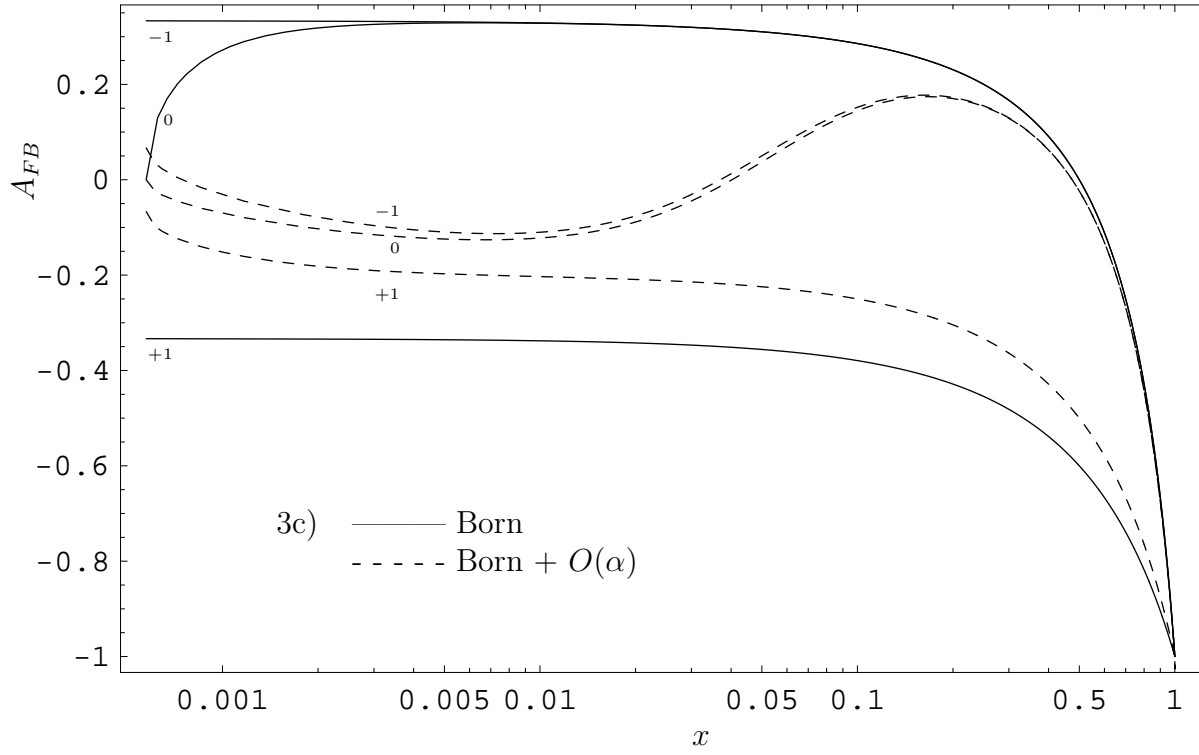


2c) ——— Born
 - - - - - Born + $O(\alpha)$

Figures 2a,b,c:

The case $\tau \rightarrow \mu$. Caption as in Fig. 1.





3c) — Born
 - - - Born + $O(\alpha)$

Figures 3a,b,c:

The case $\tau \rightarrow e$. Caption as in Fig. 1.